2007 IEEE International Conference on
Robotics and Automation
Roma, Italy, 10-14 April 2007

Control Method for Surgical Robot to Prevent Overload at Vulnerable Tissue

Yo Kobayashi, Takeharu Hoshi, Kazuya Kawamura and Masakatsu G. Fujie, *Members, IEEE*

Abstract— **Organs have many vulnerable tissues such as blood vessels and nerves which must never be damaged. This paper shows a control method which prevents the overload of vulnerable tissues. Firstly, the force control method, which prevents overload, is shown. Secondly, a FEM-based stress obsever using the organ model is described. Finally, a control method incorporating the first and second steps, and which prevents overload at vulnerable tissue, is shown. Based on the experimental result of positional and stress data; it is shown that the stress at vulnerable tissues didn't widely exceed limit stress, in the event that a target position potentially resulting in damage to vulnerable tissue was ordered.**

I. Introduction

In recent years, research and the development of technology, such as surgical robots and navigation systems, achieving minimally invasive surgery, has been carried out in various fields [1-2]. Since surgical robots achieve more minimally invasive and precise surgery than conventional surgical equivalents, they can enhance patients' early recovery. Expectations of surgery performed by minimally invasive surgical robots have increased, and research and development into surgical robot systems has advanced in many fields [3-4].

A. Motivation

Organs have many blood vessels and nerves which must never be damaged. The organs are prone to become deformed, due to contact and pushing coming from the surgical robot, since the organs are soft. This leads to regions housing nerves or blood vessels, which are especially vulnerable to overloads, becoming deformed. With this in mind, it is necessary to conduct surgical tasks while preventing the stressed state from reaching dangerous levels, especially in zones containing vulnerable tissue such as blood vessels and nerves.

In order to carry out such safe surgery, it is necessary to observe the stress state of organ. Because stress loaded on the organ is not obtained by any sensor, physical organ model is necessary to estimate these information. In order to achieve this concept, our group has reported the stress evaluation of brain using a 2D-Finite Element Method (FEM) organ model [5]. In that paper, only stress evaluation was carried out for surgical navigation.

In this paper, we target a control method for minimizing damage to tissue by robotic manipulation during surgery. For realizing this purpose, we propose an organ model-based observer of tissue damage based on intra-operative force measurements and the control method concerning to observed stress information.

B. Previous Work

The considerable amount of previous work on force information for the surgical robot represents force feedback for the surgeon using a bilateral control. For example, P. Pitakwatchara, et al. developed a method of force feedback augmentation to improve the force perception [6]. J. Arata, et al. developed the minimally-invasive surgical system, which had performed remote surgery experiments with augmented force feedback capability [7]. Shun Wang, et al. developed the robotic system with force feedback for micro-surgery[8]. Force feedback to the surgeon will be essential for safe surgery.

Physical organ modeling has aroused considerable recent attention, with various pieces of research on this topic having been conducted by large numbers of researchers worldwide [9]. Conventional research into the modeling of living bodies mainly concerns deformation analysis using a FEM. This research mainly targets surgical simulation and training [10-12]. For example, Tiller et al. present a deformation analysis of the uterus using FEM [13] and surgical simulation analyses using FEM have been researched in previous work. For example, Alterovitz et al. have researched the simulation of needle insertion for Prostate Brach therapy [14]. Meanwhile, DiMaio et al. illustrate a system for measuring the extent of planar tissue phantom deformation during needle insertion, through a linear elastic material model [15]. These works focus on analyzing the overall deformation of the target organ.

In previous work, the force feedback method for the surgeon was researched and many organ models, upon which deformation analysis was conducted, were researched for surgical planning and training. These surgical systems present

Manuscript received September 15, 2006. This work was supported in part by the 21st Century Center of Excellence (COE) Program "The innovative research on symbiosis technologies for human and robots in the elderly dominated society", Waseda University, Tokyo, Japan ,and in part by "Establishment of Consolidated Research Institute for Advanced Science and Medical Care", Encouraging Development Strategic Research Centers Program, the Special Coordination Funds for Promoting Science and Technology, Ministry of Education, Culture, Sports, Science and Technology, Japan and in part by "the robotic medical technology cluster in Gifu prefecture," Knowledge Cluster Initiative, Ministry of Education, Culture, Sports, Science and Technology, Japan.

Y. Kobayashi, T. Hoshi, K. Kawamura are with Graduate School of Science and Engineering, Waseda University, Japan, Shinjuku-ku, Ohkubo, 3-4-1 (phone:+81-3-5286-3412; fax: +81-3-5291-8269; e-mail: you-k@ fuji.waseda.jp).

Masakatsu G. Fujie is with Graduate School of Science and Engineering, Waseda University, and Faculty of Science and Engineering, Waseda University, Japan.

information concerning the displacement of the targeted organ. We target the development of an organ model to observe tissue stress based on intra operative force measurements and we also target the development of control method based on "stress" feedback to the surgical robot to prevent overload at vulnerable tissue. The integration of organ model-based stress observer and stress control method prevent the overload at vulnerable tissues.

C. Technical Problem

In this paper, we target a control method for a surgical robot based on the organ model, which prevents overload at vulnerable tissues. The following three steps are considered:

1) A control method preventing overload: In order to prevent overload, a force control method, in which the loaded force is limited to a certain value, is necessary. This control method is also required to enable precise positioning, because it is an important advantage and feature of a surgical robot.

2) Real time stress observation: In order to obtain the stress information of the vulnerable internal tissue, stress observation method by organ model is required. The stress observer must be in real time because the calculated stress is used for the manipulator control.

3) The integration: In order to prevent overload at vulnerable tissues, the manipulator must exert control to avoid the stress level exceeding the breaking point. The use of control preventing overload using estimated stress makes this possible.

The flow of this paper is listed as follows:

a) Methods (Chapter 2)
b) Experiments (Chapter 3)
c) Results and Discussions (Chapter 4)
d) Conclusions and Future Work (Chapter 5)

II. METHODS

This chapter shows the control method illustrated in this paper. Firstly, the force control method, which prevents overload, will be shown. Secondly, the stress calculation using the organ model will be described. Finally, a control method incorporating the first and second steps, and which prevents overload at vulnerable tissue, will be shown.

A. Position/Limited Force Control Method

Overload may be caused when only a position control is used when the force exerted on the organ is not taken into consideration. Force control, for example compliance control or impedance control, is conventionally used when the robot comes into contact with the target object.

However, the simple uses of these methods result in constant position errors because the surgical robot functionally touches the organ and exerts force. This renders the conventional impedance or compliance control ineffective because the surgical robot is required for precise positioning.

The control methods for surgical robots require both prevention of overload and position precision. This section shows a control method realizing both precise positioning and the prevention of overload. We have named the control method "Position/Limited Force control".

In surgical situation, position precision is required when the loaded force is small, while prevention of overload is required when the loaded force is large.

The force don't exceed breaking point when force is controlled to the target force set to the approximate value. Thus, the force control to approximate force is used to prevent the overload.

The idea behind realizing both position precision and prevention of overload is to conduct a change of control method. The position control is used when the loaded force is small, while force control to prevent overload is used when the loaded force is large. However, simple change of control method causes the unstable state such as oscillation.

Thus, we propose transition of control mode from position control to force control as the force increases. The control method we propose is separated into two parts, position control part and transition part. The switching of control is decided by the mode change force f_c. The mode change force f_c is controller parameter which is decided considering the stiffness or breaking strength of target tissue. The position control is used when the loaded force don't exceed the mode change force f_c, while the control to prevent overload is used when the loaded force exceed the mode change force f_c. The general position control is used in the position control part. The control method in transition part is described as follows in details:

1) Transition method from position control to force control: The impedance control is the method which decides the virtual impedance of the manipulator. The equation of the impedance control is shown in (1).

$$m\Delta\ddot{p} + c\Delta\dot{p} + k\Delta p = -\Delta f$$
$$\Delta p = p_t - p,\ \Delta f = f_t - f \tag{1}$$

where p is the position of the manipulator, f is the force exerted by the manipulator, p_t is the target position of the manipulator ordered by the master manipulator, f_t is the target force, and m, c, k represent the parameters of impedance control.

The impedance parameter k in (1) indicates the virtual stiffness of the manipulator movement. Equation (1) turns to position control when stiffness k is infinite. Moreover, (1) turns to force control when stiffness k is zero. Therefore, the transition of control method from position control to force control is made possible using such variable stiffness control.

In (1), the manipulator position p and the force loaded with manipulator f represents the state of the manipulator, and target position p_t is ordered by the master manipulator. Therefore, the approximate setting of the target force and impedance parameters (m, c, k) in (1) with this information (p, f, p_t) helps achieve transition form position control to force control. The target force generation method is shown in 2) and stiffness change algorithm is described in 3).

2) Stiffness change algorithm: The stiffness of movement must be decreased and be saturated to zero to transit into force control. Thus, the stiffness k must decrease and be saturated to zero, corresponding to the increase in force. The change of

stiffness must also be smooth in order to prevent any unstable state. The example calculation of stiffness k is in (2). a Stiffness -Force diagram is shown in Fig.1.

$$k(f) = k_o e^{(f-f_c)/T_k} \quad (f > f_c) \tag{2}$$

where f is the force exerted by the manipulator, f_c is the force at mode change and k_o, T_k is the parameter of the controller.

3) Target Force Generation: Any change of target force must be smooth to prevent any unstable state. When the target force is set to be saturated to a certain load, the force is limited to the saturated force. Subsequently, the target force must remain saturated to a certain force, which is named "limited force". The example calculation of target force f_t is in (3). A Target Force - Target Position diagram is shown in Fig.2.

$$f_t(p_t) = f_c + (f_l - f_c)(1 - e^{(p_t - p_c)/T_f}) \quad (f > f_c) \tag{3}$$

where f is the force exerted by the manipulator, p_t is the target position, p_c is the position at mode change, f_c is the force at mode change, f_l is the limited force, and T_f is the parameter of the controller.

Then, the Position/Limited Force control is calculated by (4) using (1), (2), and (3).

$$m\Delta\ddot{p} + c\Delta\dot{p} + k(f)\Delta p = -(f_t(p_t) - f) \tag{4}$$

B. Organ Model-based Stress Observer

When solving model, constraints in position or/and in force are applied to the surface of model. In a general approach,

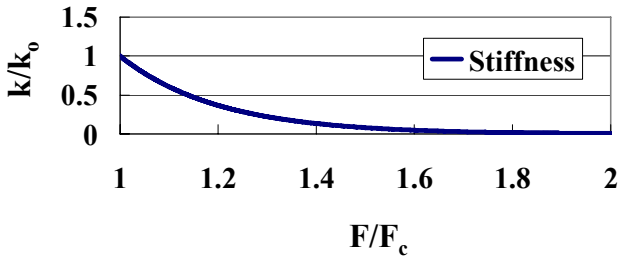

Fig.1.
This figure shows an example Stiffness-Force diagram, where the graph is separated into two parts by mode change force. The stiffness decreases and is saturated to zero.

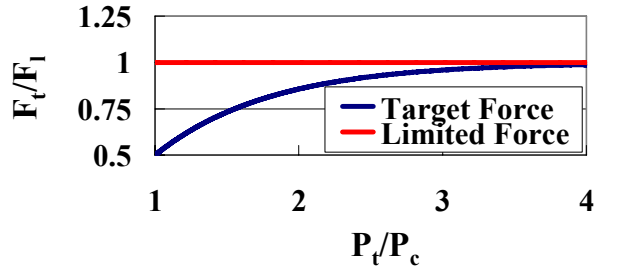

Fig.2.
This figure shows an example Target force–Target position diagram, the target force is saturated to the limited force.

constraints in position is used for solving model because boundary condition are mainly the contact point displacement between the surgical tool and the organ model. However, use of constraints in position have the problem with registration and collision detection for intra-operative stress observation.

Registration between pre-planned model and real organ derive certain level of error and the registration error cause stress observation error, while collision detection is complex and well known problem in surgical simulation [16]. Thus, we use force information measured by the force sensor for constraints in force. This section shows organ model-based stress observer using measurement force.

The Finite Element Method (FEM) based organ model is used for stress observation. In the FEM, the expression between the displacements at all the nodal points and all the applied loads is shown by the matrix calculation in (5) and (6).

$$F = KU \tag{5}$$

where **F** is the external force vector, **K** is the overall stiffness matrix, and **U** is the overall displacement (deformation) vector.

$$U = CF$$
$$C = K^{-1} \tag{6}$$

where **C** is the inverse stiffness matrix, called flexibility matrix.

Since the estimated stress is used to control the manipulator, the simulation speed must be kept very high. A condensation technique is used for real time calculation. We use the condensation technique described in, for example [10]. The stress observation process using condensation technique is described as follows:

Firstly, the external force is only considered to be exerted on the surface node. Equation (6) is divided into matrix and vector block represented by (7).

$$\begin{Bmatrix} U_s \\ U_i \end{Bmatrix} = \begin{bmatrix} C_{ss} & C_{si} \\ C_{is} & C_{ii} \end{bmatrix} \begin{Bmatrix} F_s \\ F_i \end{Bmatrix} \tag{7}$$

where subscript s stands for the surface node blocks and subscript i – for the inner node block.

The condensation can be carried out because $\mathbf{F_i}$ is the zero vector.

$$\begin{Bmatrix} U_s \\ U_i \end{Bmatrix} = \begin{bmatrix} C_{ss} \\ C_{is} \end{bmatrix} \{F_s\} \tag{8}$$

Secondly, it is considered that the necessary nodal displacement is only of the specific elements which express vulnerable tissues. Equation (8) is divided into a matrix and a vector block represented by (9).

$$\begin{Bmatrix} U_{sn} \\ U_{sv} \\ U_{in} \\ U_{iv} \end{Bmatrix} = \begin{bmatrix} C_{ssn} \\ C_{ssv} \\ C_{isn} \\ C_{isv} \end{bmatrix} \{F_s\} \tag{9}$$

where the subscript n stands for the node blocks at normal tissue and subscript v – for the node blocks at vulnerable tissues.

The condensation can be carried out because only stress loaded with vulnerable tissues is required.

$$\begin{Bmatrix} U_{sv} \\ U_{iv} \end{Bmatrix} = \begin{bmatrix} C_{ssv} \\ C_{isv} \end{bmatrix} \{F_s\} \tag{10}$$

The relationship matrix between overall nodal displacement vector and the overall stress component vector is decided using (11).

$$\{\Sigma_v\} = [\Gamma_v]\{U_v\} \tag{11}$$

where **Σ** is the overall stress component vector, **U** is the overall displacement vector of nodal position, and **Γ** is the relationship matrix between overall nodal displacement and overall stress component.

We obtain the (12) using (10) and (11).

$$\begin{aligned} \{\Sigma_v\} &= [T]\{F_s\} \\ [T] &= [\Gamma_v]\begin{bmatrix} C_{ssv} \\ C_{isv} \end{bmatrix} \end{aligned} \tag{12}$$

where subscript v stands for the node blocks at vulnerable tissues, **Σ** means the overall stress component vector, **T** means relationship matrix between overall external force vector and overall stress component. Matrix **T** is named "the stress transfer matrix," and **Γ** means the relationship matrix between the overall nodal displacement and the overall stress component.

Stress transfer matrix **T** is used for the stress observation of the manipulator controller and the stress exerted on vulnerable tissue is calculated in terms of the force exerted by the manipulator into (12).

C. Position/Limited Stress Control

In this section, a control method ensuring stress does not exceed the breaking point is shown. The position/limited force control method described in section A, and using the observed stress shown in section B, is used to achieve this. In order to prevent overload of each element, the stress of all vulnerable tissue elements must be lower than the breaking point. With this in mind, it is necessary to ensure the peak stress in all vulnerable tissue elements does not exceed the breaking stress.

To evaluate the tissue stress state, Von-Mises equivalent stress is used. Von-Mises equivalent stress at plane stress is represented as (13).

$$\sigma_v = \sqrt{\frac{1}{2}\left\{(\sigma_1-\sigma_2)^2+(\sigma_2-\sigma_3)^2+(\sigma_3-\sigma_1)^2\right\}} \tag{13}$$

where σ_1, σ_2, σ_3 is the principal stress.

The largest stress used in the control at the vulnerable element is defined as (14).

$$\sigma_{\max} = \max_{\{v\}}(\sigma_v) \tag{14}$$

where σ_{max} *is* the largest stress, σ_v is the Von-Mises equivalent stress at each vulnerable tissues.

The step of the Position/Limited Stress control is listed as follows. Firstly, the stress state at all vulnerable tissue is calculated by (12); using force information exerted by the manipulator. Then, the Von-Mises equivalent stress at each vulnerable tissue is obtained by (13). The largest stress σ_{max} is used for the manipulator control and then the Position/Limited Stress control is calculated in (15). The block diagram of the control system is shown in Fig.3.

$$m\Delta\ddot{p} + c\Delta\dot{p} + k(p_t)\Delta p = -(\sigma_t(\sigma_{\max}) - \sigma_{\max}) \tag{15}$$

III. Experiments

In this chapter, an experiment concerning Position/Limited Stress control is carried out.

A. Manipulator

This section shows the manipulator used in the experiment (Fig.4). The experimental manipulator has three degrees of freedom achieving planner movement. Three serial joints achieve a position with two translation degrees of freedom and one rotation degree of freedom respectively. The position of the manipulator is controlled with individual joint controls, the movement of which is decided by inverse kinematics. Each joint is driven by a DC motor controlled using a PID controller. A six-axis force/torque sensor (NANO 1.2/1, BL AUTOTEC) is attached to the root of the third joint and the surgical tool is attached to the six-axis force/torque sensor. The force and torque information loaded for the surgical tool are measured by the sensor. For the experiment, the surgical tool shown in Fig.4, is used to push the experimental target.

B. Phantom

The silicone is used for the organ phantom in the experiment. In this section, the phantom shape and its boundary condition are shown.

1) Shape: the phantom was made into a rectangular solid, with two types of silicone rubber used. One silicone rubber was used to create a mock-up of the parenchyma of the organ. The other was a mock-up of a fragile organ section, i.e. incorporating blood vessels or nerves. The fragile silicone section, which is softer than the others, is in the inner part of the phantom and surrounded by parenchyma silicone.

2) Boundary Condition: the lower and upper sides of the phantom are wedged between the experimental base and the acrylic plate, while the rear side of the phantom is constrained by the wall. The boundary condition of the phantom is shown in Fig.5. A dimensional outline drawing of the phantom is shown in Fig.5, and Fig.6 illustrates a picture of the same.

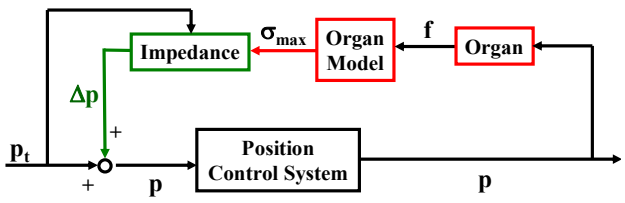

Fig. 3.
This figure shows the block diagram of control system. The largest stress σ_{max} is observed by organ model and is used for the manipulator control. The stiffness of impedance controller is decided by the target position p_t and largest stress σ_{max}.

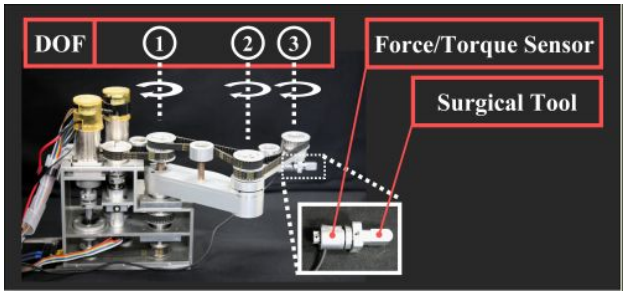

Fig. 4.
This figure shows the manipulator used in this experiment. The experimental manipulator has three degrees of freedom achieving planner movement. A six axis load cell is attached and the force information exerted by the manipulator is sensed.

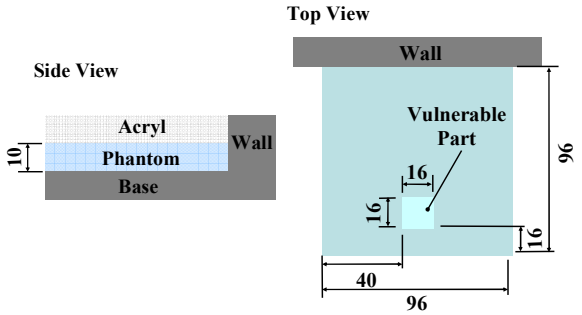

Fig. 5.
This figure shows side and top views of the phantom shape. Softer silicone rubber (mock-up of the fragile part of an organ) is included within harder silicone rubber (mock-up of parenchyma of the organ).

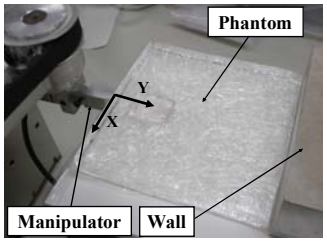

Fig. 6.
This figure depicts the experimental setup.

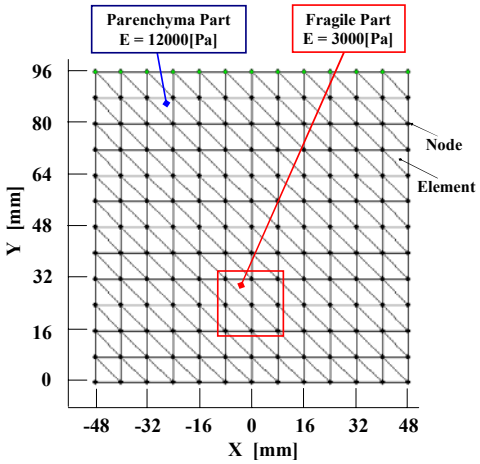

Fig. 7.
This figure shows the initial shape of the FEM organ model. A 2-D slice of the organ model is defined using mesh triangular elements. The figure shows the dimensional outline drawing of the model. The total node number of this model is 169 and the total element number is 288.

TABLE I
PARAMETERS OF PHANTOM MODEL

Phantom	Elastic modulus	Stress limit
parenchyma	$1.2 * 10^4$[Pa]	$5.0 * 10^3$ [Pa]
vulnerable tissue	$3.0 * 10^3$[Pa]	$7.5 * 10^2$ [Pa]

C. *Organ Model Realization*

Tissue deformation is complex and remains the subject of much research [17-18]. In general, tissue modeling is complex because of its inhomogeneous, non-linear, and anisotropic elastic and viscous behavior. As an initial approximation, this study focuses on homogeneous, linear elastic models that estimate the stress state in two dimensions. Since the silicone used in this experiment has an almost elastic and homogenous body, it correlates to the aforementioned assumption.

Linear FEM is used for the organ model in this experiment and a 2-D slice of the organ model is defined using mesh triangular elements (Fig.7). The shape of the model is designed to be similar to the phantom. The inner part simulating vulnerable tissue is included in the model, which has an elastic modulus lower than others. Table 1 shows the tissue parameters, such as elastic modulus, and stress limit. The stress observation process is mainly divided into two parts, where one involves offline calculation carried out before the experiment and the other involves online calculation carried out during the experiment respectively.

1) Offline-calculation: Firstly, the stiffness matrix of each triangular element is calculated, and then the overall stiffness matrix is decided by adding the stiffness of all elements adjacent to the nodal point and taken into consideration. The flexibility matrix (inverse stiffness matrix) is obtained by the inverse matrix calculation of the stiffness matrix. Moreover, the γ matrix for each element is also calculated for (11), following which the condensation method from (7) to (12) is implemented, subsequently leading to the stress transfer matrix at (12) being obtained. The stress transfer matrix **T** is sent to the manipulator controller.

2) Online-calculation: The stress is observed by (12) during experiment, using information from the force sensor. The force information from the force sensor is divided into forces exerted at each nodal point, following which the stress at each vulnerable element is observed.

D. *Experimental Condition*

In this section, the experimental condition is shown. A situation whereby the command from the master manipulator has the potential to exert dangerous stress on vulnerable tissues is assumed. The manipulator is ordered to push the phantom in the Y direction and is then controlled using the position/limited stress control method. The Y position of the ordered target increases linearly, by 10 mm relative to the target position. The experiment is repeatedly carried out, changing the X coordinate of the pushing point. (X coordinates of the pushing point are -36,-28,-20,-12, -4, 4, 12, 20, 28 and 36 mm)

The limited stress σ_l is set to be 750 Pa and the stress at mode change σ_c is set to be 500 Pa in this experiment.

IV. Results And Discussions

A. Position and Stress Data

In this section, the experimental result of stress data involving Position/ Limited Stress control is shown. Figure 8 shows the result of the largest stress σ_{max} when the Position/ Limited Stress control method is implemented.

When the σ_{max} is small, the result shows the position is nearly equal to the target position, and the force increase corresponds to the increase in the target position. The stress σ_{max} also increases in line with the target position.

When the σ_{max} is large, the result shows a halt to the increase in the position, while the target position continues increasing, meaning the force is saturated to a certain value. The stress σ_{max} also stops increasing and becomes saturated to the stress limit while the target position increases.

These results show that the stress σ_{max} does not widely exceed the stress limit in the case that a target position potentially leading to damage of vulnerable tissue is ordered. On the other hand, positional precision is realized when a small amount of stress is exerted.

B. Difference in the Pushing Position

In this section, the change of acceptable force is shown. Figure 9 shows the force exerted by the manipulator at each pushing point of X coordinate, when the stress limit σ_l is exerted on a certain vulnerable tissue.

The experimental result shows a considerable acceptable load when the pushing position of coordinate X is far from the vulnerable tissue and a small acceptable load when the pushing position X is near. This is because the force caused by the contact is largely transmitted from the surface to the vulnerable tissue when the pushing position of coordinate X is near while little force is transmitted when the pushing position of coordinate X is far. These results, in which the acceptable force changes based on the pushing position of coordinate X, show that simply using the force information obtained by the force sensor alone is insufficient. Stress evaluation at the organ itself is necessary, in order to prevent overload of vulnerable tissues.

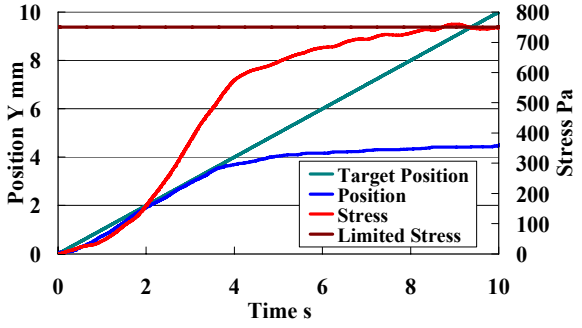

Fig. 8.
This figure shows the experimental result of the largest stress σ_{max} and the force loaded with manipulator F_s. This figure shows the stress σ_{max} does not exceed the stress limit where a target position potentially damaging to vulnerable tissue is selected.

C. Overall Deformation and Stress Distribution

The evaluation of the overall organ state is also important for safe surgery [5]. In this section, the overall organ deformation and stress distribution during the experiment are evaluated. To evaluate the stress, the safety margin, which is defined by the ratio of stress to the Limited Stress σ_l is used. Figure 10 shows the overall deformation and distribution of the safety margin when the Limited Stress is exerted. Fig.10 (1) is the result when the pushing point X is 4 mm and, (2) is 12 mm, (3) is 20 mm respectively.

The following sentences show the discussion of each result of this experiment:

1) Near position (X = 4mm): Figure 10(1) shows that the stress increase was mainly apparent in the vulnerable tissue area and that while sight change was visible in the surrounding area, only little stress was apparent elsewhere. The vulnerable tissue area is deformed largely in forward and reverse directions and is displaced into the reverse direction.

2) Middle position (X = 12mm): Figure 10(2) shows that the stress increase was mainly apparent in the vulnerable tissues. Moreover, although slight change was shown in the right reward area of the vulnerable tissue and the pushing point, only little stress was evident elsewhere. The right side of the vulnerable tissue area was deformed mainly in forward and reverse directions and displaced into the reverse and left directions.

3) Far position (X = 20mm): Figure 10(3) shows that the stress increase was mainly apparent in the area of vulnerable tissues and the pushing point. Moreover, although slight change was shown in the right reward area of the vulnerable tissue and the pushing point, only little stress was evident elsewhere. The right side of the vulnerable tissue area was deformed mainly in forward and reverse directions and displaced into the reverse and left directions. Dangerous stress is shown at the pushing position in the result of Fig.10 (3), which shows the potential for overload at the surface tissue of the organ. Therefore, this result shows the necessity for stress evaluation in the vicinity of the pushing point, such as the vulnerable tissue area described in this paper, in order to prevent damage of the surface tissue.

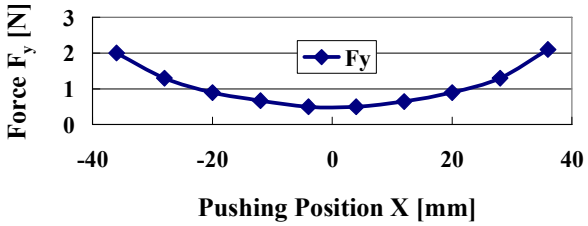

Fig. 9.
This figure shows the force exerted by the manipulator at each pushing point of X coordinate when the Limited Stress σ_l is exerted on a certain vulnerable tissue. The acceptable force is changed by the pushing position of coordinate X.

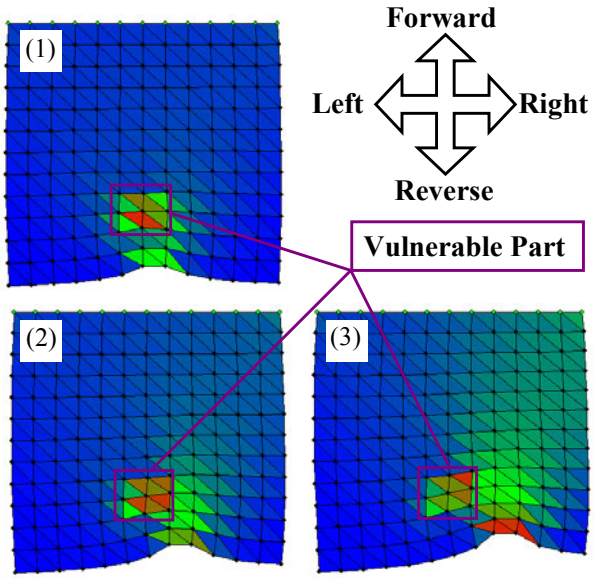

Fig. 10.
This figure shows the overall deformation and distribution of the safety margin when Limited Stress is exerted. The color of each element switches from blue, green to red corresponding to the increase in the safety margin. The color of the element is red when the safety margin exceeds 1. The change in the tendency of stress distribution and deformation at vulnerable tissue is shown from these figures.

V. Conclusions and Future Work

A control method intended for a surgical robot, which prevents the overload of vulnerable tissues using force information, is shown in this paper. Firstly, Position/Limited Force control, which is a control method achieving both precise positioning and prevention of overload was illustrated. Secondly, a stress observation method involving an organ model using FEM, and its condensation technique of calculation, was shown. Finally, this paper showed a Position/Limited Stress control, in which estimated stress was used for the Position/Limited Force control. Based on the experimental result of positional and stress data; it is shown that the stress σ_{max} didn't widely exceed stress limit in the event that a target position potentially capable of damaging vulnerable tissue, was ordered. On the other hand, positional precision was achieved with only little stress exerted. In consideration of the pushing point, the necessity for stress evaluation at the phantom to prevent overload at vulnerable tissues is described. Then, the result of the overall stress distribution and deformation is shown.

In future work, further precise modeling of organ will be carried out. For example, 3D organ model will be developed and viscoelastic and nonlinear characteristics as reported in [17] [18] will be included to organ model. Moreover, acquisition of organ geometries, for example as reported in [5], will be researched for actual applications. Model parameter identification method using intra-operative information will be researched to concern ambiguity of model parameter. Using these control methods, a surgical robot achieving safe and precise surgery will be developed.

References

[1] Intuitive Surgical, http://www.intuitivesurgical.com

[2] K.Hongo, Y.Kakizawa, J.Koyama, K.Kan, K.Nishizawa, F.Tajima, M.G.Fujie, and S.Kobayashi, "Microscopic-manipulator system for minimally invasive neurosurgery -Prelininary study for clinical application-", Proceedings of the 15th Congress and Exhibition of Computer Assisted Radiology and Surgery, pp.265-269 (2001)

[3] R. H. Taylor and D. Stoianovici "Medical Robotics in Computer-Integrated Surgery", IEEE Transaction on Robotics and Automation,Vol. 19, No. 5 (2003)

[4] P. Daraio, B. Hannaford and A. Menciassi, "Smart Surgical Tools and Augmenting Devices", IEEE Transaction on Robotics and Automation Vol. 19, No. 5 (2003)

[5] Aiko Yoshizawa, Jun Okamoto, Hiroshi Yamakawa,Masaktsu G. Fujie "Robot Surgery based on the Physical Properties of the Brain-Physical Brain Model for Planning and Navigat ion of a Surgical Robot-" , In IEEE International Conference on Robotics and Automation (2005)

[6] P. Pitakwatchara, S. Warisawa, M. Mitsuishi, "Automatic Determination of the Action for the Improvement of Force Perception in the Minimal Invaisive Surgical System", In IEEE International Conference on Intelligent Robotics and Systems (2005)

[7] J. Arata, H. Takahashi, P. Pitakwatchara, S. Warisawa, K. Konishi, K. Tanoue, S. Ieir, S. Shimizu, N. Nakashima, K. Okamura, Y. S. Kim, S. M. Kim, J. S. Hahm, M. Hashizume and M. Mitsuishi, "A remote surgery experiment between Japan-Korea using the minimally invaisive surgery system", In IEEE International Conference on Robotics and Automation (2006)

[8] S. Wang, J. Ding and J. Yun, Q. Li and B. Han, "A Robotic System with Force Feddback for Micro-Surgery", In IEEE International Conference on Robotics and Automation (2005)

[9] The IUPS Physiome Project, http://www.bioeng.auckland.ac.nz/physiome/physiome_project.php

[10] V. DANIULAITIS, M.Osama ALHALABI, H. KAWASAKI, Yu Tanaka and T. HORI , "Medical Palpation of Deformable Tissue using Physics-Based Model for Haptic Interface RObot", In International Conference on Intelligent Robots and Systems (2004), 3907-3911

[11] Steffen Markle,Alla Gothan and Holger Gothan "Interactive Simulation of Soft-Tissue for Surgery Training" In Computer Assisted Radiology and Surgery (1999) 855-859

[12] U.Meier, F.J.Garcia, N.C.Parr, C.Monserrat, J.A.Gil, V.Grau, M.C.Juan and M.Alcaniz "3D surgical trainer with force feedback in minimally invasive surgery" In Conputer Assisted Radiology and Surgery (2001) 33-39

[13] Y.Tillier, A.Paccini, M.Durand-Reville, F.Bay and J.L.Chenot "Three-dimensional finite element modeling for soft tissues surgery" In Conputer Assisted Radiology and Surgery (2003)

[14] R. Alterovitz, A. Lim, K. Goldberg, G. S. Chirikjian, and A. M. Okamura, "Steering Flexible Needles under Markov Motion Uncertainty", In International Conference on Intelligent Robots and Systems (2005)

[15] S.P.DiMaio and S.E.Salcudean "Needle Insertion Modelling and Simulation", In IEEE Transaction on Robotics and automation ,Vol. 19, No. 5, 2003

[16] M.BRO-NIELSEN, "Finite Element Modeling in Surgery Simulation", In Proceedings of the IEEE, Vol.86, No.3, March (1998), 490-503

[17] Yo Kobayashi, Jun Okamoto, Masaktsu G Fujie "Physical Properties of the Liver and the Development of an Intelligent Manipulator for Needle Insertion" , In IEEE International Conference on Robotics and Automation (2005)

[18] Yo Kobayashi, Jun Okamoto, Masaktsu G Fujie "Physical Properties of the Liver for Needle Insertion Control" , In IEEE International Conference on Intelligent Robotics and Systems (2004)